Preparation of Supercapacitor Electrode from Gasified Rice Husk Carbon

Huilin Wang,[a,b] Dajun Wu,[b] Jianbin Zhou,[a,*] Huanhuan Ma,[a] Deliang Xu,[a] Bin Qian,[b] Shi Tao,[b] and Zhe Wang [a]

Various biomass resources have been fabricated and devoted to the application of energy storage. Rice husk is a promising candidate for a supercapacitor, but its conductivity and surface to weight ratio are much poorer than commercial activated carbon. In this paper, the byproduct of rice husk gasification power generation as a raw material was boiled with KOH solution and activated by CO_2 to prepare activated carbon. The authors selected the appropriate activation temperature and lye mass fraction to prepare the activated carbon electrode. A scanning electron microscope was used to characterize the surface topography. The porosity of the carbon was detected by nitrogen adsorption. The electrochemical behavior was determined by using galvanostatic charge-discharge, cyclic voltammetry, and impedance spectroscopy techniques. When the activation temperature was 850 °C and the mass fraction of the KOH solution was 30%, the Brunauer-Emmett-Teller specific surface area of the activated carbon reached a maximum value of 1383 m^2/g and the specific capacitance was 168 F/g at 250 mA/g with good electrochemical performance.

Keywords: Gasified rice husk carbon; Activated carbon; KOH; Specific capacitance

Contact information: a: College of Materials Science and Engineering, Nanjing Forestry University, Nanjing 210037, China; and b: Changshu Institute of Technology, Changshu 215500, China;
**Corresponding author: whl@cslg.edu.cn*

INTRODUCTION

With the development of human society, biomass energy, and new energy, storage devices, such as supercapacitors, have received widespread attention as green energy because of their fascinating prospects (He *et al.* 2013; Li *et al.* 2016). The electrode materials play a key role on the performance and price of supercapacitors (Bin-Hai *et al.* 2017). All kinds of materials with good conductivity and high specific surface can be used as supercapacitor electrode materials, including carbon materials, metal oxides, metal hydride materials, and conductive polymer materials, *etc.* Activated carbon is still considered the most potential application of electrode materials, and it has been applied in commercial capacitors (Jiang *et al.* 2009; Min *et al.* 2015; Ruquan *et al.* 2015). However, the existing commercial activated carbon is prepared from coal, asphalt, and petroleum coke as raw material. The raw material of the prepared activated carbon is non-renewable (Liu *et al.* 2016).

Rice husk is cheap and has a large amount of biomass resources that can be used to generate electricity or the preparation of syngas, bio-oil, and activated carbon (Shen *et al.* 2014). The yield of gasified rice husk carbon is higher than 20%. Gasified rice husk carbon contains a certain amount of disordered aromatic rings and graphite-like structure (Zhu *et al.* 2015), which have potential to facilitate charge storage in electrode materials of the

supercapacitor. The byproduct of rice husk gasification power generation as the electrode material of the supercapacitor has promising potential. Herein, a unique and facile method is presented to convert gasified rice husk carbon into activated carbon, in which the samples are boiled by KOH solution to remove silicon oxide (Yeletsky *et al.* 2009), and co-activated by KOH and CO_2 to prepare activated carbon with appropriate micropores and mesoporous pores. The as-prepared activated carbon with micropores and mesopores shows superior capacitance, good conductivity, and excellent rate capability. The roles of boiling KOH solution and activated CO_2 in the process of gasified rice husk carbon were analyzed. This work offers a universal method to prepare unique active carbon materials from gasified rice husk carbon for various important energy storage systems.

EXPERIMENTAL

Materials

The gasified rice husk carbon was obtained from Anhui Xinquan Rice Co., Ltd. of Hefei, China, which included 49.3 wt% charcoal, 4.4 wt% volatile, and 46.3 wt% ash. The gasified rice husk carbon was washed and dried at 103 °C for 8 h, and then was smashed and sieved to pass through a 200 mesh screen for further use, and recorded as 'RHC'.

Methods

Preparation of activated carbon

The RHC was used as a raw material, and a KOH solution with a mass fraction of 5% according to a 1:10 (w/v) solid-liquid ratio was added. They were mixed with an electric stirrer and boiled at 110 °C for 1 h. Subsequently, the obtained solid product was calcinated under a CO_2 atmosphere at either 800 °C, 850 °C, or 900 °C for 1 h using tube furnace (Model OTL1200, Nanjing University Instrument Factory, Nanjing, China), respectively. The activated carbon was first washed with distilled water, then immersed with 0.5 M hydrochloric acid, and finally washed with boiling distilled water to a neutral pH. After desiccating for 4 h, activated carbons with different activation temperatures were marked as RHC8005, RHC8505, and RHC9005.

The RHC was used as a raw material and the solid/liquid ratio was kept in the same way as the first step. Then, KOH solution of 5%, 15%, 30%, and 40% were added, mixed with an electronic stirrer, and filtrated after being boiled at the temperature of 110 °C for 1 h. Subsequently, the obtained solid product was calcinated under a CO_2 atmosphere at 850 °C for 1 h. The activated carbon was washed with distilled water, and then immersed in 0.5 M hydrochloric acid. Next, the activated carbon was washed with boiling distilled water until the pH was neutral. The resulting activated carbon was dried in a vacuum oven for 4 h and labeled as RHC8505, RHC8515, RHC8530, and RHC8540, which dealt with 5%, 15%, 30%, and 40% KOH solution, respectively. The heating and cooling process were in the N_2 atmosphere with the rate of 10 °C/min.

Characterization

The activated carbon surface area and pore size distribution were analyzed through an automatic surface area and pore size analyzer Q10 automatic analyzer (Quantachrome Corporation, Boynton Beach, FL, USA). Using N_2 as an adsorbent, an adsorption isotherm was obtained at 77 K with a Q10 automatic analyzer. The Brunauer-Emmett-Teller (BET) and the density functional theory (DFT) methods were used to calculate the specific surface

area and pore size distribution, respectively. The surface morphology of activated carbon was measured by a field emission scanning electron microscope JSM-7600F (JEOL Ltd., Tokyo, Japan).

Electrochemical measurements

The electrode was prepared by mixed activated carbon that was uniformly milled. The binder was polyvinylidene fluoride (PVDF), and the sp-type carbon black was dispersed in N-methylpyrrolidone with a mass ratio of 80:10:10 (Chen *et al*. 2017), which was then pasted on the nickel foam and dried in the vacuum oven at 80 ℃ overnight. The loaded mass of activated carbon was 5 mg/cm^2. The cyclic voltammetry (CV), galvanostatic charge and discharge (GCD) and alternating current (AC) impedance were carried out at the CHI760E electrochemical workstation (Chenhua, Shanghai, China) with the active carbon electrode as the working electrode, the platinum electrode as the counter electrode, and the saturated calomel electrode as the reference electrode (Song *et al.* 2015). The electrolyte was 6 M KOH aqueous solution. The mass specific capacitance at different charge and discharge current densities was determined according to Eq. 1,

$$C = I \cdot t / (m \cdot \Delta V) \quad (1)$$

where C is the specific capacitance (F/g), I is the discharge current (A), t is the discharge time (s), m is the mass of the active materials in the single electrode (g), and ΔV is the potential difference (V) in the discharge process (Lazzari *et al.* 2007).

RESULTS AND DISCUSSION

Activated Carbon Specific Surface Area and Pore Size

Figure 1 shows the SEM images of the activated carbon prepared by KOH boiling and CO_2 activation from gasified rice husk carbon. As shown in Fig. 1, the prepared activated carbon was a porous material with many pores on the surface, which enhanced the specific surface, thus increasing the specific capacitance as active materials of the supercapacitor electrode.

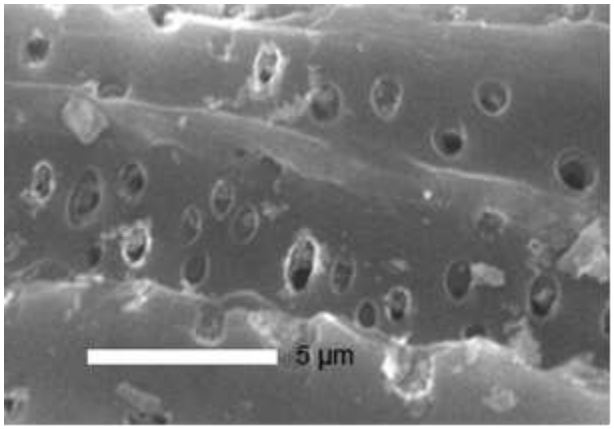

Fig. 1. SEM image of activated carbons prepared from gasified rice husk carbon

Table 1. BET Surface Area and Pore Parameters of Activated Carbons

Sample	BET Surface Area ($m^2 \cdot g^{-1}$)	Pore Volume ($mL \cdot g^{1}$)	Average Pore Diameter (nm)
RHC8005	623	0.37	2.10
RHC9005	590	0.59	2.69
RHC8505	648	0.39	2.41
RHC8515	764	0.68	2.56
RHC8530	1383	1.02	2.95
RHC8540	1064	1.68	3.97

Additionally, the nitrogen adsorption-desorption measurements were further performed to investigate the specific surface area and pore size parameters of the samples (Table 1). When the mass fraction was 5%, with the increase of activation temperature, the specific surface area first increased and then decreased, which showed that an appropriate activation temperature could develop specific surface area, thus increasing electrode materials/electrolyte interface surface to enhance specific capacitance. When the activation temperature was 850 °C, with increased mass fraction, the specific surface area showed the same trend. The total pore volume and the average pore size were 2 mL/g and 3 nm, respectively. Micropores and mesopores co-existed in the activated carbon. However, excessive temperature and a higher concentration of KOH resulted in porosity reduction, which also led to the collapse of holes (Yu *et al*. 2013). Some of the micropores were turned into mesopores, and some mesopores were converted into macropores. The pore volume and average aperture increased as well. When the activation temperature was 850 °C and the mass fraction of KOH was 30%, the maximum specific surface area was 1383 m^2/g.

The N_2 isothermal adsorption curves of the samples prepared at different mass fractions at 77 K are shown in Fig. 2. With increased KOH mass fraction, the adsorption capacity of activated carbon first was high, and then it decreased. The mass fraction of 30% had the best adsorption performance. However, when the mass fraction increased to 40%, the adsorption performance decreased because the porous network connectivity in activated carbon were destroyed by the excessive concentration KOH solution.

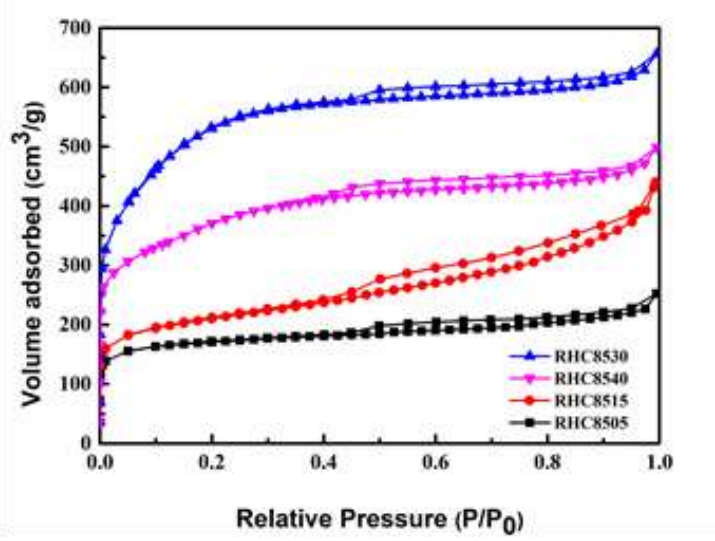

Fig. 2. N_2 isothermal adsorption curve of activated carbon prepared at different KOH mass fractions

When the relative pressure (P/P_0) was less than 0.1, the adsorption capacity of the sample rapidly increased, which indicated a well-developed microporous structure. In addition, capillary condensation occurred on the adsorbate, and this led to the desorption isotherm above the adsorption isotherm resulting in an adsorption lag (hysteresis), which indicated a certain amount of mesoporous present. When the relative pressure (P/P_0) exceeded 0.95, the adsorption amount rapidly increased again, the adsorption saturation could not be reached at high pressure, and the adsorption desorption hysteresis loop appeared (Kuppireddy *et al.* 2014). According to IUPAC classification, the adsorption type belonged to type I + type IV, and there were a lot of micropores and a certain amount of mesoporous in the activated carbon.

The pore size distributions of the samples prepared by different mass fractions are as shown in Fig. 3. The results showed that the average pore size of RHC8540 was the largest and RHC8540 had the highest proportion of mesopores, as shown in Table 1.

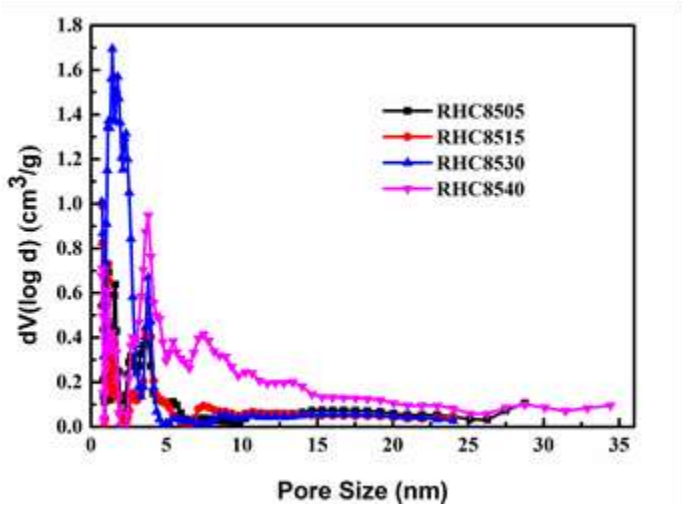

Fig. 3. Pore size distribution of the activated carbon calculated by DFT methods

Electrochemical Properties

Cyclic voltammetry

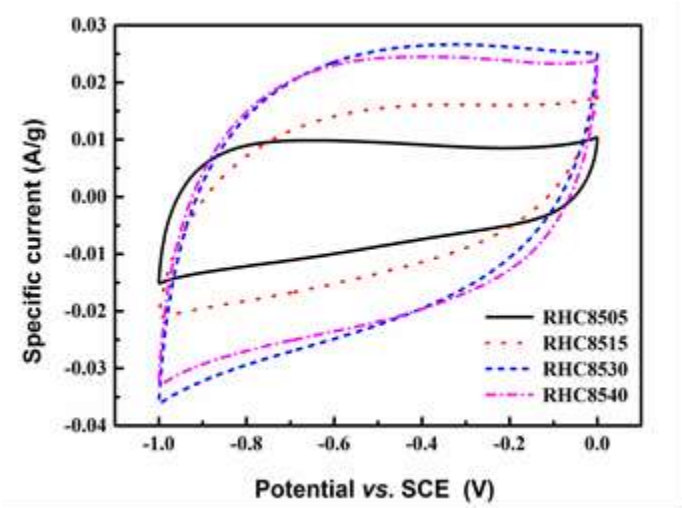

Fig. 4. CV curves of activated carbons at different KOH mass fraction (-1 V to 0 V, 20 mV/s)

Figure 4 shows the CV curve of the four active carbon electrodes within the voltage range of -1 V to 0 V at 20 mv/s. An increased mass fraction of the boiling solution led to an increased curve area in the same sweep speed. All four curves had no obvious redox peaks. They possessed a roughly rectangular shape, which illustrated that the electrode had good stability and low internal resistance.

AC impedance characteristics

An EIS test can study the electrochemical system AC impedance changes with the frequency (Wu *et al.* 2016); the complex plan reflects the impedance characteristics of the electrode system (Wen *et al.* 2013). The frequency range of AC impedance tests for 4 kinds of active carbon electrodes is from 0.1 Hz to 100 kHz, and the direct current (DC) bias voltage is 0. As shown in Fig. 5, the impedance spectra and equivalent circuit were obtained by complex nonlinear least square fitting. The equivalent series resistance (ESR) (R_1) was 0.56 Ω, 0.71 Ω, 0.49 Ω, and 0.51 Ω for samples RHC8505, RHC8515, RHC8530, and RHC8540, respectively. The R_1 value of RHC8530 was slightly smaller than that of the other samples because of the larger specific surface contact area and appropriate porous structure. The diameter of the arc corresponded to the Faradic charge transfer resistance (R_2); therefore, the smaller R_2 of sample RHC8530 (0.28 Ω) compared to the others (1.01 Ω, 0.43 Ω, 2.14Ω) illustrated more rapid adsorption/desorption at the electrode-electrolyte surface due to outstanding ion transport and electron conduct. A straight line with a slope of 45° in the low frequencies that arose from accumulation of ions at the bottom of the pores in the electrode demonstrated better capacitive behavior with diffusion limitation (Wu *et al.* 2015).

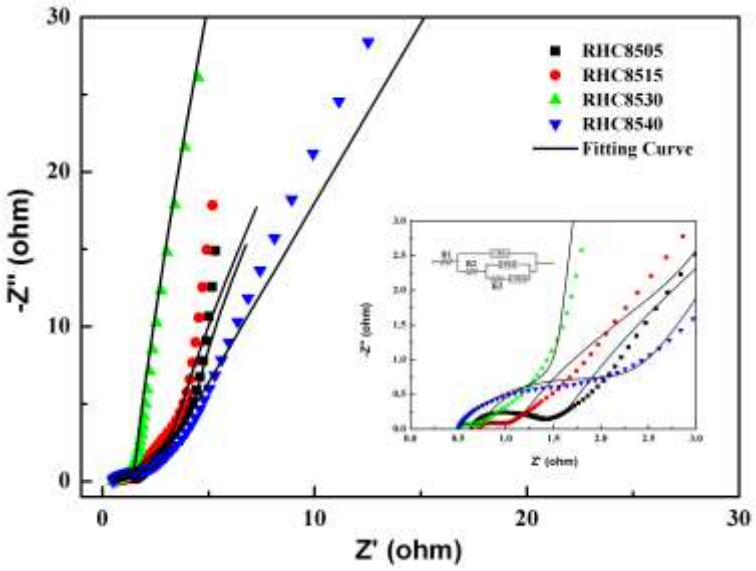

Fig. 5. The electrochemical impedance spectroscopy (EIS) of activated carbons prepared at different KOH mass fraction

Constant current charge and discharge performance

The galvanostatic charge-discharge test of samples was conducted in a voltage range of -1 v to 0 v. It was clear that the charging-discharging curves of four kinds of activated carbon electrodes at 0.25 A/g roughly formed a triangle, and the charging curve and discharging curve were generally symmetrical. The d*E*/d*t* value presented a linear

relationship, which showed its good capacitance. Moreover, a greater voltage drop failed to appear at the moment of the reversal of current, which showed that the equivalent series resistance of the four activated carbon electrodes was low. Meanwhile, RHC8530 had the largest specific capacitance. According to the charging-discharging curve, the specific capacitance of RHC8505，RHC8515，RHC8530, and RHC8540 electrodes discharging was 115 F/g, 144 F/g, 168 F/g, and 141 F/g, respectively. The RHC8505, RHC8515, and RHC8530 curves showed that the specific capacitance increased with increased specific surface area. Furthermore, the RHC8540 charging curve and discharging curve were not exactly symmetrical, which revealed that the charge resistance was large.

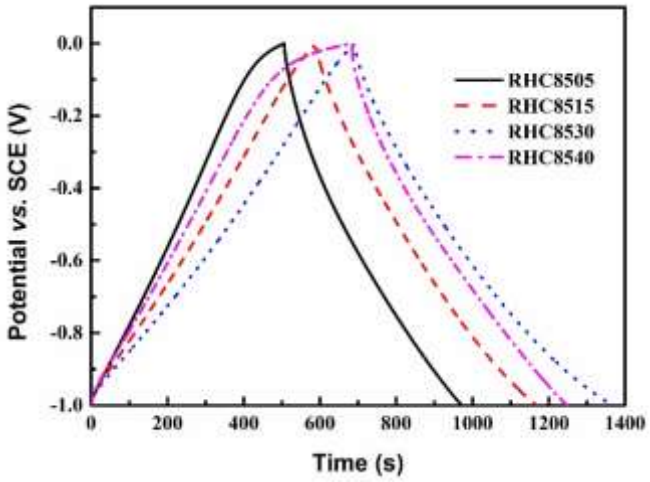

Fig. 6. The charge and discharge curves of activated carbon electrode prepared at different KOH mass fraction (-1 V to 0 V, 250 mA/g)

High current with fast charge and discharge is one of the prominent advantages of supercapacitors, and these features distinguished them from the performance of batteries. Therefore, the high current rate performance of carbon electrode materials is particularly important. The high current performance of RHC8530 in 6 M KOH is shown in Figs. 7. and 8.

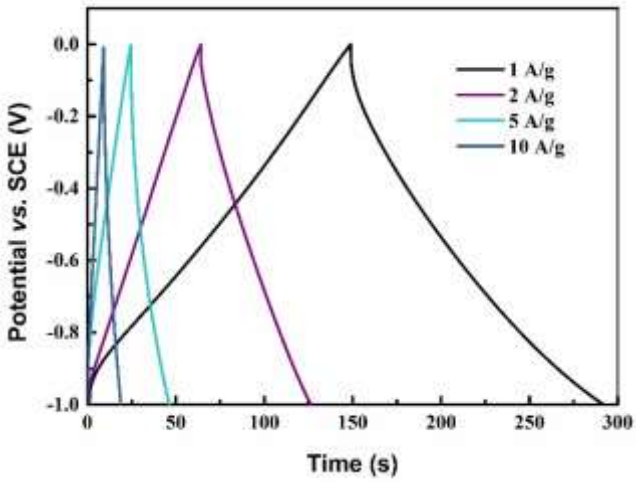

Fig. 7. The charge-discharge curve of the RHC8530 electrode at different current densities

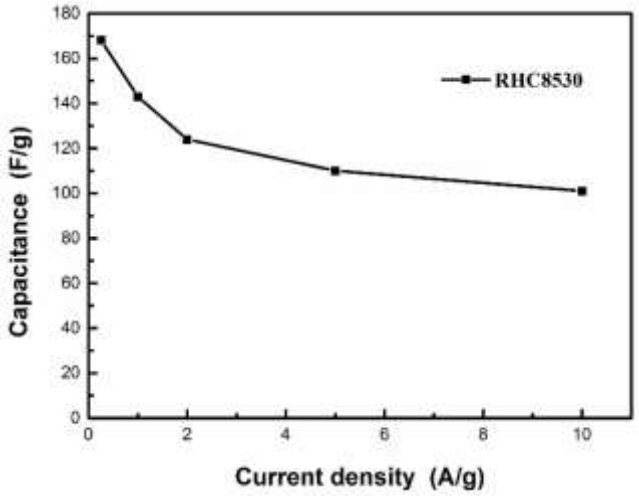

Fig. 8. Rate performance of RHC8530 in 6 mol·L^{-1} KOH electrolyte

Under the large current density, the mass specific capacitance of RHC8530 decreased with increased current density, which was calculated as 143 F/g, 124 F/g, 110 F/g, and 101 F/g at 1 A/g, 2 A/g, 5 A/g, and 10 A/g, respectively, and showed that the specific capacitance slowly decreased. The current density increased from 1 A/g to 10 A/g, and the specific capacitance of RHC8530 remained at 101 F/g, whose retention rate was as high as to 71%, indicating that the RHC8530 had relatively good charge and discharge performance, and better rate performance.

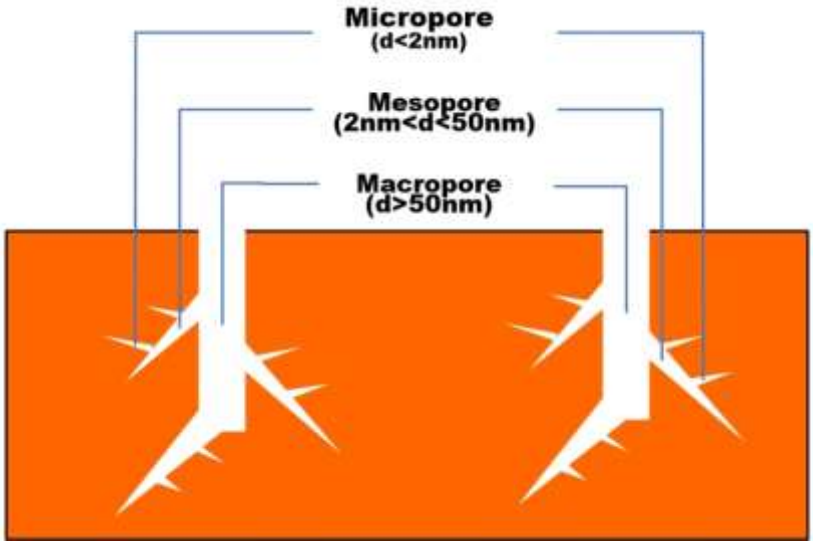

Fig. 9. Porous carbon models of RHC

According to the definition of IUPAC, the pores of porous carbon can be classified into three groups: micropores (d < 2 nm), mesopores (2 nm < d < 50 nm), and macropores (d > 50 nm) (see Fig. 9). As shown in Figure 9，abundant pores structure may be present in RHC. Macropores can be seen in SEM (Fig. 1), whereas mesopores and micropores can be reflected in BET (Table 1). This helps to further comprehend the construct of gasified rice husk carbon clearly with the good electrochemical performance. The unique

micropores and mesoporous structure of RHC as electrochemical active sites not only enhance specific surface area but also support the enough accommodation for electron conduct and fast ionic transportation channels, obtaining high electrochemical performance.

CONCLUSIONS

Gasified rice husk carbon as a raw material paired with KOH boiling and CO_2 activation was examined, and the activation temperature and lye mass fraction on the preparation of activated carbon was discussed.

1. Activated carbon contained micropores and mesoporous pores. When the KOH mass fraction was 30% and activation temperature was 850 °C, RHC8530 had a specific surface area of 1383 m^2/g and a specific capacitance of 168 F/g in 6 M KOH electrolyte.
2. The current density increased from 1 A/g to 10 A/g, the specific capacitance was maintained at 101 F/g, and the retention rate was as high as 71%. The RHC8530 had good capacitance retention, good CV, and good EIS characteristics, which can be used as a supercapacitor electrode material.

ACKNOWLEDGEMENTS

This work was supported by the National Natural Science Foundation of China (51776100), the Priority Academic Program Development of Jiangsu Higher Education Institutions (PAPD), and the National Key Research and Development Plan of China (2016YFE0201800).

REFERENCES CITED

Bin-Hai Cheng, R. J. Z. H. (2017). "Recent developments of post-modification of biochar for electrochemical energy storage," *Bioresource Technology* 246, 224-233. DOI: 10.1016/j.biortech.2017.07.060

Chen, J., Zhou, X., Mei, C., Xu, J., Zhou, S., and Wong, C. (2017). "Evaluating biomass-derived hierarchically porous carbon as the positive electrode material for hybrid Na-ion capacitors," *Journal of Power Sources* 342, 48-55. DOI: 10.1016/j.jpowsour.2016.12.034

He, X., Ling, P., Yu, M., Wang, X., Zhang, X., and Zheng, M. (2013). "Rice husk-derived porous carbons with high capacitance by $ZnCl_2$ activation for supercapacitors," *Electrochimica Acta* 105, 635-641. DOI: 10.1016/j.electacta.2013.05.050

Jiang, X. M., MO, C., Bin, X., and Shan, H. S. (2009). "Spherical activated carbon prepared by NaOH activation as electrode materials for supercapacitors," *Electronic Components & Materials* 28(8), 59-61. DOI: 10.3969/j.issn.1001-2028.2009.08.017

Kuppireddy S K R, Rashid K, Al Shoaibi A, Srinivasakannan C (2014). "Production and characterization of porous carbon from date palm seeds by chemical activation with H_3PO_4: Process optimization for maximizing adsorption of methylene blue,"

Chemical Engineering Communications 201(8), 1021-1040. DOI: 10.1080/00986445.2013.797896

Lazzari, M., Mastragostino, M., and Soavi, F. (2007). "Capacitance response of carbons in solvent-free ionic liquid electrolytes," *Electrochemistry Communications* 9(7), 1567-1572. DOI: 10.1016/j.elecom.2007.02.021

Li, H., Sun, Z., Zhang, L., Tian, Y., Cui, G., and Yan, S. (2016). "A cost-effective porous carbon derived from pomelo peel for the removal of methyl orange from aqueous solution," *Colloids and Surfaces A: Physicochemical and Engineering Aspects* 489, 191-199. DOI: 10.1016/j.colsurfa.2015.10.041

Liu, D., Zhang, W., Lin, H., Li, Y., and Lu, H. (2016). "A green technology for the preparation of high capacitance rice husk-based activated carbon," *Journal of Cleaner Production* 112(1), 1190-1198. DOI: 10.1016/j.jclepro.2015.07.005

Min, H., Xian-Lun, D., Kang, S., Feng-Long, X., and Hua, Y. (2015). "Research progress of activated carbon as electrode material for supercapacitor," *Biomass Chemical Engineering* 49(3), 59-64. DOI: 10.3969/j.issn.1673-5854.2015.03.011

Ruquan, R., Tongxin, S., Xiaojuan, J., and Chen, J. (2015). "Nitrogen-enrich activated carbons from waste particleboard as electrodes for electric double layer capacitor," *Journal of Northeast Forestry University* 43(12), 93-98. DOI: 10.13759/j.cnki.dlxb.20151116.006

Shen, Y., Zhao, P., and Shao, Q. (2014). "Porous silica and carbon derived materials from rice husk pyrolysis char," *Microporous and Mesoporous Materials* 188, 46-76. DOI: 10.1016/j.micromeso.2014.01.005

Song, S., Ma, F., Wu, G., Ma, D., Geng, W., and Wan, J. (2015). "Facile self-templating large scale preparation of biomass-derived 3D hierarchical porous carbon for advanced supercapacitors," *Journal of Materials Chemistry A* 3(35), 18154-18162. DOI: 10.1039/C5TA04721H

Wen, B., Wei, S., Shi, Z., Lin, H. B., and Lu, H. Y. (2013). "Capacitance performance and model analysis of activated carbon derived from rice husks," *Chemical Journal of Chinese Universities* 34(3), 674-678. DOI: 10.7503 /cjcu20120481

Wu, D., Xu, S., Li, M., Zhang, C., Zhu, Y., Xu, Y., Zhang, W., Huang, R., Qi, R., Wang, L., and Chu, P. K. (2015). "Hybrid MnO_2 /C nano-composites on a macroporous electrically conductive network for supercapacitor electrodes," *Journal of Materials Chemistry A* 3(32), 16695-16707. DOI: 10.1039/C5TA03938J

Wu, D., Xu, S., Zhang, C., Zhu, Y., Xiong, D., Huang, R., Qi, R., Wang, L., and Chu, P. K. (2016). "Three-dimensional homo-nanostructured MnO_2/nanographene membranes on a macroporous electrically conductive network for high performance supercapacitors," *Journal of Materials Chemistry A* 4(29), 11317-11329. DOI: 10.1039/C6TA01823H

Yeletsky, P. M., Yakovlev, V. A., Mel Gunov, M. S., and Parmon, V. N. (2009). "Synthesis of mesoporous carbons by leaching out natural silica templates of rice husk," *Microporous and Mesoporous Materials* 121(1-3), 34-40. DOI: 10.1016/j.micromeso.2008.12.025

Yu, W., Xiao-Juan, J., and Zhang, J. (2013). "Characteristics of nitrogen-enriched activated carbon prepared from waste medium density fiberboard by potassium hydroxide," *Journal of Wood Science* 59(2), 133-140. DOI: 10.1007/s10086-012-1312-4

Zhu, L., Yin, S., Yin, Q., Wang, H., and Wang, S. (2015). "Biochar: A new promising catalyst support using methanation as a probe reaction," *Energy Science and Engineering* 3(2), 126-134. DOI: 10.1002/ese3.58

Article submitted: December 20, 2017; Peer review completed: April 8, 2018; Revised version received: April 13, 2018; Accepted: April 21, 2018; Published: April 26, 2018.
DOI: 10.15376/biores.13.2.4279-4289